

Development of the 3D Shape Shearography Technique for Strain Inspection of Curved Objects

Anisimov, Andrej; Serikova, M.G.; Groves, Roger

DOI

[10.1364/DH.2016.DTh3C.4](https://doi.org/10.1364/DH.2016.DTh3C.4)

Publication date

2016

Published in

2016 Imaging and Applied Optics Congress

Citation (APA)

Anisimov, A., Serikova, M. G., & Groves, R. (2016). Development of the 3D Shape Shearography Technique for Strain Inspection of Curved Objects. In *2016 Imaging and Applied Optics Congress: Heidelberg, Germany* OSA Publishing. <https://doi.org/10.1364/DH.2016.DTh3C.4>

Important note

To cite this publication, please use the final published version (if applicable). Please check the document version above.

Copyright

Other than for strictly personal use, it is not permitted to download, forward or distribute the text or part of it, without the consent of the author(s) and/or copyright holder(s), unless the work is under an open content license such as Creative Commons.

Takedown policy

Please contact us and provide details if you believe this document breaches copyrights. We will remove access to the work immediately and investigate your claim.

Development of the 3D Shape Shearography Technique for Strain Inspection of Curved Objects

Andrei G. Anisimov^{*1}, Maria G. Serikova², Roger M. Groves¹

¹*Aerospace Non-Destructive Testing Laboratory, Delft University of Technology,
Kluyverweg 1, 2629 HS, Delft, The Netherlands*

²*Department of Optical-Electronic Devices and Systems, ITMO University,
Kronverksky 49, Saint Petersburg, 197101, Russia
a.g.anisimov@tudelft.nl*

Abstract: Practical development questions of 3D shape shearography technique for surface strain inspection of curved objects are discussed. Results of a global cameras-projector system calibration and different methods of shear distance estimation in 3D are presented.

OCIS codes: 120.6165, 120.4630, 120.2650, 150.3040, 110.4190

1. Introduction

Shearography (speckle pattern shearing interferometry) is a coherent-optical inspection technique [1, 2] often used for non-destructive testing (NDT) and strain measurement [2, 3]. Being an imaging technique, shearography provides full field measurements in a non-contact way. Shearography directly measures the surface displacement gradients which give a quantitative estimate of in- and out-of-plane surface strain components [2, 3]. Six surface strain components, including in- and out-of-plane components can be measured with known 3D shearography configurations (with three or more viewing or illumination directions) [3, 4].

The surface strain components can be measured if the information about the object, its shape and location, is known. Mostly flat objects at a known distance were inspected before [2, 3]. In case of a flat object the data processing procedure can be significantly simplified and processing can be done in a “2D manner”. However, if the object is curved, its shape and location have to be measured. The shape information is required for correction of the shear distances within the field of view [2, 5] together with sensitivity vector correction [2]. A general solution to the strain inspection of curved objects was reported before [6]. The 3D shearography setup was equipped with an integrated structured light projector for inline shape measuring. That is why the technique was called 3D shape shearography. The complete procedure of the 3D shape shearography system calibration and data processing were also presented [6]. Current research follows the earlier work [6, 7] and is devoted to crucial practical questions of the 3D shape shearography system development. This includes ways to estimate the shear distance in 3D and the camera-projector system calibration. This paper covers in brief these practical questions.

2. 3D shape shearography technique for strain inspection of curved objects

During measurements with shearography a speckle pattern is generated by illuminating a rough surface with an expanded laser beam. Speckle patterns are recorded with a camera with a shearing device (Fig. 1 (a)) before and after the surface deformation (e.g. thermal or mechanical loading). The shearing device duplicates the camera field of view (FOV) so that a reference and sheared FOV are shifted one from another. If a Michelson interferometer is used in the shearing device, one of the mirrors introduces this shear (Fig. 1 (a)). In case of a non-planar surface the shear distance d_i varies along the surface. However, the actual value of the shear distance d_i for each surface point i is needed for calculation of the surface strain components.

During the measurements two sets of interferograms are captured before and after the surface deformation. A phase-shift algorithm [8] can be used to obtain phase differences from these sets. Correlation analysis of the phase differences before and after the deformation results in a phase change which contains information on the surface displacement gradients. The developing 3D shape shearography technique uses a multiple viewing approach with three shearing cameras and a single illumination direction (Fig. 1 (b)) [6, 9]. Simultaneous use of three cameras is needed to isolate the in- and out-of-plane surface strain components [2, 4].

The earlier proposed approach [6] for surface strain measuring of curved objects by the 3D shape shearography is used in this research. The approach is based on transferring shearography data from the system to each point of the point cloud, which can be done in 4 steps:

1. Inline object shape measuring with integrated structured light projector.
2. Estimation of the shear distances in x - and y -directions in 3D for each shearing camera.
3. Conventional shearography: capturing phase shifted interferograms before and after the object deformation, phase change obtaining and processing (incl. filtering, 2D unwrapping and zero order fringe tracking) [2, 3].

4. Transferring all the shearography data (phase, shear distances in x - and y -directions and sensitivity vectors) from all cameras to each point of the cloud to calculate the strain components at each particular point.

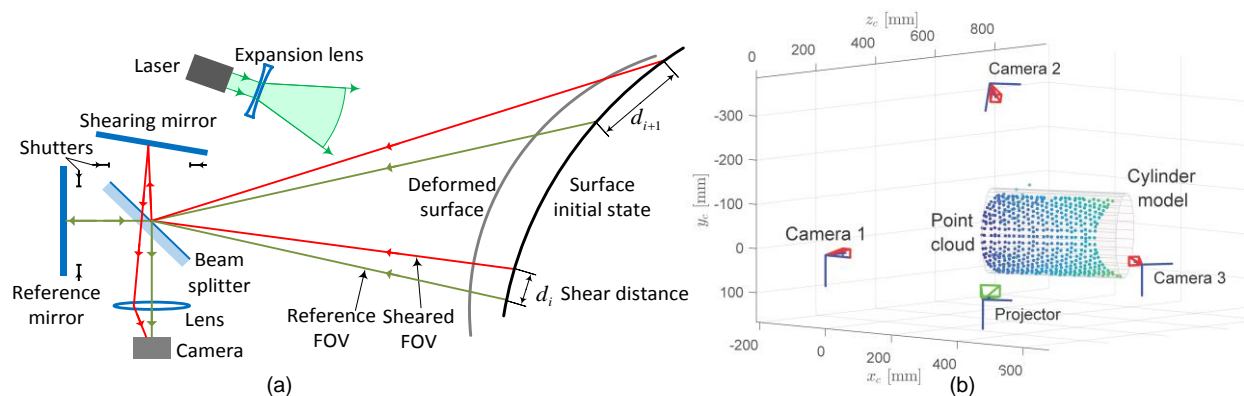


Fig. 1. 3D shape shearography: (a) schematic representation of the shearing camera and the shearing device based on a Michelson interferometer, (b) result of cameras-projector geometry calibration together with a point cloud corresponding to a cylinder specimen and a fitted cylinder model.

3. Global calibration of the 3D shape shearography system

For the step 1 (shape measuring), the cameras and the projector require geometric calibration. The well-known Zhang's camera model [10] can be used for this purpose. Previously in [6] the cameras and the projector were calibrated in pairs as stereovision systems [11, 12]. Recently global calibration of the cameras and the projector (as an inverse camera) was done using the multiple view computer vision approach [13]. First, the cameras intrinsic parameters were identified in a conventional way [14]. Then, a global optimisation procedure was done to identify the extrinsic parameters of the cameras and the projector [13]. As a result, a reprojection error for the three cameras was less than 2.7 pixels (RMS). Reprojection error defines the overall spatial resolution of the 3D shape shearography technique when phase values from three cameras are combined at each point of the point cloud.

The calibration is done for the reference optical paths of shearing cameras when the shutters in the shearing arm of each interferometer are blocked (Fig. 1 (a)). The shape of the object can be measured with the common phase-shifting technique by projecting sinusoidal fringes onto the object [15] and presented as a point cloud (Fig. 1 (b)).

4. Shear estimation in 3D

Earlier it was proposed [6] to estimate the shear distance for each data point P of the cloud (Fig. 2) by projecting it to each camera C , identifying the shear in the image space pq and reprojecting it back to the surface. The intersection of \overline{Cq} with the surface gives a point Q which is a corresponding "sheared" point for the initial point P . Shear in the camera space can be estimated by digital image correlation [16] of images captured independently first, through the reference field of view, and then through the sheared one (Fig. 1 (a)).

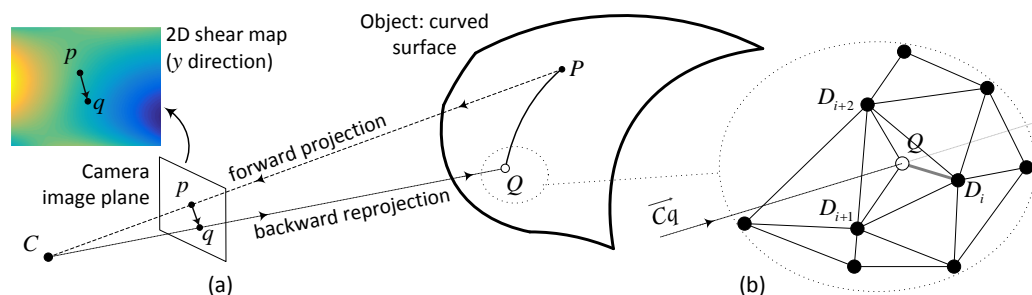


Figure 2. Estimation of the shear distances in 3D:

(a) forward projection and backward reprojecting and (b) intersection of the "sheared" ray with the object's surface.

To get the shear distance PQ , the point Q has to be discovered. This was done by searching the nearest to the ray \overline{Cq} point of the cloud (e.g. D_i in Fig. 2 (b)) [6]. However, this simple approach results in areas with a step rises of the shear (Fig. 3 (a)). The points of the point cloud correspond to pixels of the camera. As pixels have a linear discrete structure, points of the cloud also have some degree of regularization. When an initially smooth shear map (Fig. 2 (a)) is reprojected to the point cloud point-by-point, this regularization introduces step rises in the shear distances.

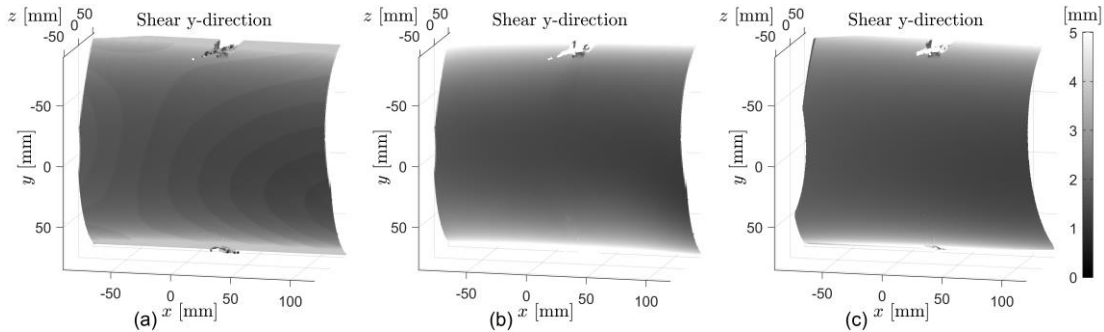


Figure 3. Shear distances in 3D estimated for camera 1 in the y -direction: (a) by searching the "nearest point of the point cloud", (b) by intersection with a fitted cylinder model and (c) by triangulation of the intersection within each facet.

If the object has a simple shape, a parametric surface can be fitted to the point cloud and the intersection of the ray \overline{Cq} with this surface can also be found parametrically [17, 18]. In case of a cylinder (Fig. 1 (b)), a cylinder model was fitted into the data points using the RANSAC algorithm [19]. Results of the parametric shear calculation are presented in Fig. 3 (b). Another approach is to identify a triangle which contains the intersection with the ray \overline{Cq} (e.g. $D_i D_{i+1} D_{i+2}$ in Fig. 2 (b)) and to triangulate the intersection point within this triangle [20]. Triangulated shear distances are shown in Fig. 3 (c).

Comparison of the shear maps obtained with the parametric (Fig. 3 (b)) and triangulation approaches (Fig. 3 (c)) shows no significant difference. The triangulation approach is more general as no surface fitting is required. As said before, the "nearest point" resulted in regions with a step rises of the shear distance. The same step rises are expected in the surface strain components, as the shear distances are directly used for the strain calculation.

3. Conclusions

Practical development questions of the 3D shape shearography technique for surface strain inspection of curved objects are discussed. A global calibration of the cameras-projector system resulted in a low reprojection error, so high spatial resolution of the 3D shape shearography is expected. Three ways of shear estimation in 3D were compared. Fitting of a parametric surface together with the triangulation approach provide more accurate results than a previously used "nearest point" criteria. The obtained results will be used for further development of the 3D shape shearography technique following the aim of bringing the technique closer to a practical use in a real life.

4. References

- [1] Y.Y. Hung, "Shearography: a new optical method for strain measurement and non-destructive testing," *Opt. Eng.* 21, 213391 (1982).
- [2] W. Steinchen, L. Yang, *Digital Shearography* (SPIE, 2003).
- [3] D. Francis, R.P. Tatam, R.M. Groves, "Shearography technology and applications: a review," *Meas. Sci. Technol.* 21, 102001, 29 (2010).
- [4] R.M. Groves, S.W. James, R.P. Tatam, "Multi-component shearography employing four measurement channels," in *Proc. SPIE* 4933, pp. 135-140 (2003).
- [5] R.M. Groves, S.W. James, R.P. Tatam, "Strain measurement in curved industrial components using multicomponent shearography," in *Proc. SPIE* 4398, 216 (2001).
- [6] A.G. Anisimov, R.M. Groves, "3D shape shearography with integrated structured light projection for strain inspection of curved objects," in *Proc. SPIE*, 9525:943524 (2015).
- [7] D.T. Goto, R.M. Groves, "Error analysis of 3D shearography using finite-element modelling," in *Proc. SPIE* 7718, 771816 (2010).
- [8] B.V. Dorrio, J.L. Fernandez, "Phase-evaluation methods in whole-field optical measurement techniques," *Meas. Sci. Technol.* 10, R33-R35 (1999).
- [9] A.G. Anisimov, B. Müller, J. Sinke, R.M. Groves, "Strain characterization of embedded aerospace smart materials using shearography," in *Proc. SPIE* 9435, 943524 (2015).
- [10] Z. Zhang, "Flexible camera calibration by viewing a plane from unknown orientations," in *Proc. of the 7 IEEE International Conference on Computer Vision*, 1, pp. 666-673 (1999).
- [11] J.Y. Bouguet, "Camera calibration toolbox for MATLAB" (2004).
- [12] G. Falcao, N. Hurtos, J. Massich, D. Fofi, "Projector-Camera Calibration Toolbox," <http://code.google.com/p/procamcalib> (2009).
- [13] R. Hartley, A. Zisserman, *Multiple view geometry in computer vision* (Cambridge University Press, 2003).
- [14] J. Heikkilä, O. Silvén, "A four-step camera calibration procedure with implicit image correction," in *Computer Vision and Pattern Recognition, Proceedings IEEE Computer Society Conference*, pp. 1106-1112 (1997).
- [15] S. Zhang, "Recent progresses on real-time 3D shape measurement using digital fringe projection techniques," *Opt. Laser Eng.*, 48(2), pp. 149-158 (2010).
- [16] T.W. Ng, "Shear measurement in digital speckle shearing interferometry using digital correlation," *Opt. Comm.*, 115(3), pp. 241-244 (1995).
- [17] D.L. Toth, "On ray tracing parametric surfaces," *ACM SIGGRAPH Computer Graphics* 19.3, pp. 171-179 (1985).
- [18] D. Legland, "Graphics library geom3d," <http://www.mathworks.com/matlabcentral/fileexchange/24484-geom3d> (2016).
- [19] P. H. S. Torr, A. Zisserman, "MLESAC: A New Robust Estimator with Application to Estimating Image Geometry," *Comput. Vis. Image Und.*, 78, 1, pp. 138-156 (2000).
- [20] T. Möller, B. Trumbore, "Fast, minimum storage ray/triangle intersection," *ACM SIGGRAPH Courses* (2005).